INTERFACE

royalsocietypublishing.org/journal/rsif

Research



Cite this article: Joo S, Jung S, Lee S, Cowie RH, Takagi D. 2020 Freshwater snail feeding: lubrication-based particle collection on the water surface. *J. R. Soc. Interface* **17**: 20200139

http://dx.doi.org/10.1098/rsif.2020.0139

Received: 26 February 2020 Accepted: 30 March 2020

Subject Category:

Life Sciences—Physics interface

Subject Areas:

biomechanics

Keywords:

feeding current, particle transport, peristaltic pumping

Author for correspondence:

Daisuke Takagi

e-mail: dtakagi@hawaii.edu

Electronic supplementary material is available online at https://doi.org/10.6084/m9.figshare. c.4938165.

THE ROYAL SOCIETY

Freshwater snail feeding: lubricationbased particle collection on the water surface

Soyoun Joo¹, Sunghwan Jung², Sungyon Lee³, Robert H. Cowie⁴ and Daisuke Takagi^{1,4}

Sul, 0000-0002-1420-7921; SL, 0000-0002-4118-1712; RHC, 0000-0002-2986-7092; DT. 0000-0002-9738-1414

The means by which aquatic animals such as freshwater snails collect food particles distributed on the water surface are of great interest for understanding life at the air—water interface. The apple snail *Pomacea canaliculata* stabilizes itself just below the air—water interface and manipulates its foot such that it forms a cone-shaped funnel into which an inhalant current is generated, thereby drawing food particles into the funnel to be ingested. We measured the velocity of this feeding current and tracked the trajectories of food particles around and on the snail. Our experiments indicated that the particles were collected via the free surface flow generated by the snail's undulating foot. The findings were interpreted using a simple model based on lubrication theory, which considered several plausible mechanisms depending on the relative importance of hydrostatic pressure, capillary action and rhythmic surface undulation.

1. Introduction

Snails (Gastropoda) feed on diverse resources and in diverse ways. Many are herbivores [1], while others are fungivores [2], detritivores [3,4] and carnivores that feed on carrion [1,5] and even on other snails [6,7]. Snails feed by use of a radula, a tongue-like structure supporting rows of teeth like a rasp that is protruded from the mouth and used in various ways to gather their food [8]. For example, freshwater apple snails (family Ampullariidae, notable for their large globular shells) are primarily considered as shredders and scrapers of plant material, as well as scavengers and predators of other animals [5,9,10]. However, what sets apple snails apart from other gastropods is their highly unusual mode of feeding on small particles floating on the water surface. This is the focus of the present study.

In the presence of floating food particles, apple snails move to the water surface and use their foot to collect the particles at the air—water interface [9–13]. In general, when feeding in this mode, the snail attaches at the surface to a substrate (e.g. an emergent plant) with the posterior part of its foot, while it forms a cone-shaped funnel with the anterior part of the foot. If attached to a larger emergent surface (e.g. a bridge support) it may use the substrate itself as an integral part of the funnel. The snail may also feed in this mode while floating unattached. Once the funnel is formed, it generates a current on the water surface, which draws food particles into the funnel, forming a mucous agglutination; when sufficient food particles have accumulated, the snail reaches its head over the edge of the funnel and uses the radula to ingest the bolus of food [10,11].

Researchers have been divided on the physical origin of this surface current that draws food particles into the funnel. This feeding mode was first reported in *Pomacea paludosa* [11] and termed 'ciliary feeding' because the current was thought to be generated by beating of cilia on the ventral foot surface. It was subsequently

¹Department of Mathematics, University of Hawaii at Manoa, Honolulu, HI 96822, USA

²Department of Biological and Environmental Engineering, Cornell University, Ithaca, NY 14853, USA

³Department of Mechanical Engineering, University of Minnesota, Minneapolis, MN 55455, USA ⁴Pacific Biosciences Research Center, University of Hawaii at Manoa, Honolulu, HI 96822, USA

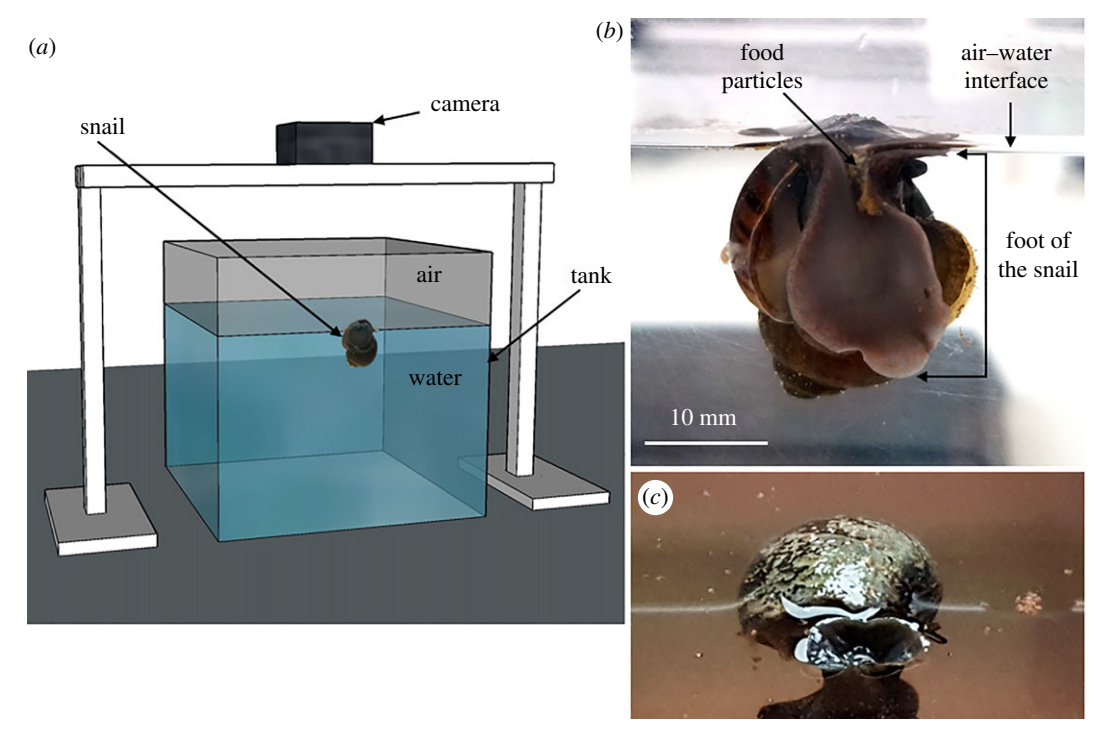


Figure 1. (a) Schematic of the experimental set-up with a single snail in a tank of water with the camera to record the motion of the food particles from above, perpendicular to the water surface. (b) Frontal view of a snail that has attached itself to the tank wall and has used the anterior part of its foot to form a funnel on the air—water interface with the wall of the tank forming part of the funnel, recorded with a second camera pointing horizontally at the snail. (c) The funnel of a free-floating snail on the air—water interface viewed from above, the anterior part of the foot forming the entire circumference of the funnel.

reported in *Pomacea canaliculata* [12], with the current attributed to rapid undulations passing posteriorly along the foot. Subsequently, ciliary movements were reported on the anterior part of the foot [9]. Recent studies [10,13] termed this feeding mode 'pedal surface collecting', a term we prefer over 'ciliary feeding' because (1) it is not clear that ciliary beating alone generates the current, rather than in conjunction with muscular wave-like contractions of the foot, and (2) 'ciliary feeding' has been generalized [14] to include all instances of gastropods using ciliary beating and mucus to collect food throughout the water column, whereas the mode of feeding considered here is specifically adopted at the air—water interface.

The above studies focused on qualitative observations. No experiments have been conducted to quantify the flow field generated by the snails during feeding, and so no studies have considered this peculiar feeding behaviour and the resultant flow from a fluid mechanics perspective. Therefore, we conducted an experimental and theoretical investigation of feeding by Pomacea canaliculata, focusing on the fluid mechanics of the observed inhalant current, rather than its physiological origin. In particular, our aim was to build and test a simple mechanistic model of pedal surface collecting, with the minimum physical components. Here, we report quantitative measurements of the particle trajectories around a feeding snail and a theoretical model of the undulating foot. This is the axisymmetric analogue of the two-dimensional flow around a snail moving along an interface [15]. The key difference is that, in our study, the snail drives the flow around it while it remains stationary. Experimental measurements show that particles floating several body lengths away from the snail are drawn towards it and collected inside the funnel. Inspired by the experimental observations, we developed a mathematical model for the dynamics of the mucous layer on the snail's foot. The model describes how the snail's foot may drive the flow of the thin mucous layer and consequently of the surrounding water. Our findings suggest possible strategies for effectively collecting particles distributed on a free surface.

2. Methods

Invasive apple snails (*Pomacea canaliculata*) were collected from Kawainui Marsh, Kaliua, on the island of Oahu, Hawaii, USA. Snails used in the experiments were mostly subadults ranging from 30 to 35 mm in shell height and 23 to 30 mm in width. They were maintained in a tank (51 cm long, 25.5 cm wide, 31 cm deep) with tap water to a depth of 19 cm, at room temperature (22–25°C) and with a natural light:dark cycle for the duration of the experimental trials, which lasted approximately 18 months. Their diet consisted of ground up 'Spectrum: Marine Fish Formula' pellets, romaine lettuce and calcium supplements.

Individual snails were isolated and starved for 2–3 days prior to video recording in a small experimental tank 26 cm by 26 cm with water 13 cm deep (figure 1a). In preparation for filming, ground fish food pellets were scattered over the entire water surface in the experimental tank. The ground pellet particles, which were approximately 1 mm in length, floated on the water surface. In most cases, the snail floated or crawled to the air–water interface and then formed a funnel with its foot. In general, the funnel formed with the anterior part of the snail's foot, while the snail attached itself to the transparent side of the tank with the posterior part of the foot. This configuration allowed the inside of the funnel to be visible through the side of the tank, which itself constituted an integral part of the funnel (figure 1b).

To capture this behaviour, two video cameras were set up, one looking vertically down onto the snail from above and the other looking horizontally through the side of the tank at the inside of the funnel (figure 1a,b). The view from above, perpendicular to the water surface, showed the snail's food collecting behaviour and permitted the tracking of food particle trajectories on the water surface. The side view showed the trajectories and location

Figure 2. (a) Food particles have been collected inside the funnel. (b,c) The snail reaches its head over the edge of the funnel and uses the radula to ingest the food. (d) Upon consumption of the food, the snail resumes its original configuration and the process is repeated.

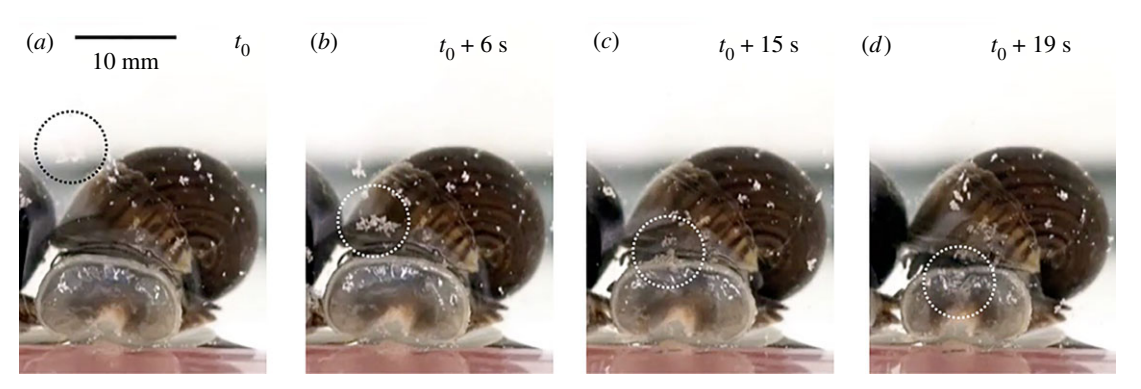


Figure 3. Time-sequential images from above. The dotted circle encloses a cluster of particles floating on the air—water interface; they move towards the undulating funnel-shaped foot over time, while the snail remains fixed in position on the tank wall. (a) A cluster of food particles has been drawn close to the snail. (b) The cluster has been drawn close to the edge of the funnel. (c) The cluster is at the edge of the funnel.

of the food particles after they entered the funnel. Videos were recorded at 29 frames per second with a resolution of up to 1920×1080 pixels (Sony Alpha 6000 and Samsung Galaxy S8). The frames were analysed using Tracker [16]. The position of each food particle was manually tracked as it moved closer to the foot over time. The velocity and radial distance from the centre of the snail's foot were determined at each frame.

3. Results and discussion

3.1. Experiments

Downloaded from https://royalsocietypublishing.org/ on 09 July 202

Time-sequence images in figure 2 illustrate the feeding cycle of the snail. Once food particles were distributed on the airwater interface, we could partition the process the snail adopted to ingest them as a series of phases. First, the foot deformed such that a part of it faced upwards and resembled a cone-shaped funnel, with the periphery of the foot extended horizontally out from the funnel across the water surface (figure 2a). Second, it maintained this configuration for a typical duration of 30 min while particles around the snail were collected within the funnel in what appeared to be an agglutination of mucus and particles. Finally, when sufficient particles were accumulated inside the funnel, the snail reached its head over the edge of the funnel and used the radula to ingest the bolus of food (figure 2b,c). Following consumption of the food particles (and emptying of the funnel), the snail resumed its funnel configuration to continue feeding (figure 2d). This process we observed reflects closely that previously described in the literature [10,11].

Hereafter, we specifically focus on the collection phase of the snail's feeding sequence and examine the flow on and around the snail as viewed from above, perpendicular to the horizontal water surface. A typical feeding sequence is shown in electronic supplementary material, video S1. During the collection phase, most of the foot and the entire shell of the snail remained submerged. Part of the underside of the foot faced vertically upwards, with a perimeter that formed almost an arc of a semicircle. The width of the topfacing edge of the foot ranged from 14 to 18 mm, and its maximum length (not just the part forming the funnel) ranged from 21 to 38 mm. Food particles as far away as 135 mm from the centre of the foot were eventually collected. Figure 3 shows the time-sequence images of the collection phase as viewed from above. A dashed open circle points to the cluster of food particles that were initially approximately 40 mm away from the funnel centre in figure 3a. Over time, food particles gradually moved towards the funnel on the air-water interface (figure 3b-d). Notably, as the particles moved, the funnel appeared to undergo surface undulations, as evident from the flickering light patterns on the funnel surface and the shape changes in the funnel edge (see electronic supplementary material, video S2). However, as noted in the Introduction, the probable presence of the funnel surface undulations does not eliminate the possibility of ciliary beating, as the two mechanisms may coexist to drive the inhalant flow towards the funnel.

Figure 4*a* shows the far-field velocity field of the inhalant current that is generated by the feeding snail. The velocity field was plotted by combining tracks of 47 particles distributed

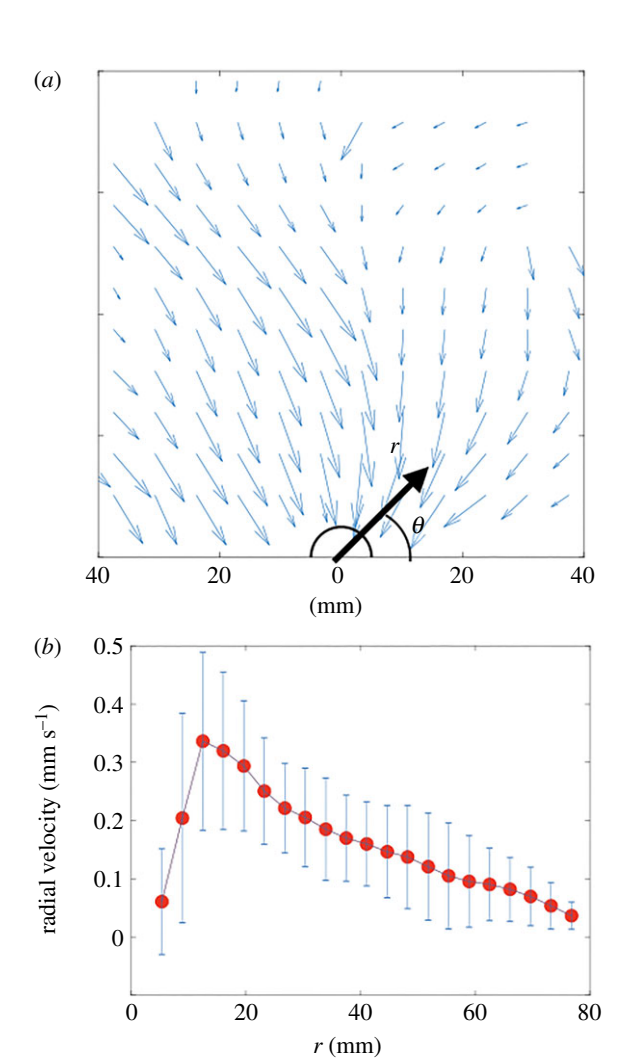


Figure 4. (a) The velocity field of particles moving towards the snail (shown as a half-circle). The length of velocity vectors was scaled up by a factor of 10. For example, an arrow length of 10 mm in the plot corresponds to 1 mm s⁻¹. (b) Radial velocity plotted as a function of the radial distance r from the funnel centre. There is a clear jump in velocity with r. As the particles move towards the snail (far field), velocity increases as r decreases, reaching a maximum at the edge of the foot. Once they reach the snail, their velocity decreases rapidly with r within the horizontal part of the funnel formed by the snail's foot (near field). Red symbols and error bars show, respectively, the mean and standard deviation of velocities from 47 particle trajectories.

randomly prior to the recording (data are tabulated in the electronic supplementary material). The particles can be interpreted as tracers of the water flow, given that the Stokes number is approximately 0.04, which is negligibly small. To generate the velocity field, we created a mesh grid of 6 mm \times 6 mm and averaged the velocities from the 47 particle trajectories in each grid. The fields varied in detail among individual snails, which created surface flows of different magnitudes and, in some cases, directions; some inhalant flows were more axisymmetric, while others exhibited distinctly asymmetric flow patterns. This explains why the averaged flow field in figure 4a is not perfectly axisymmetric. Presumably, the induced flow field depends on the size and strength of the snail, which was difficult to control in our experiments.

Regardless of individual variations, the general flow field (figure 4a) consisted of an approximately radial and inward current along the air–water interface. The magnitude of the flow becomes weaker in general with distance r from the snail as shown in figure 4b. It is difficult to deduce a functional

form for this spatial decay in the far-field velocity, mainly because of temporal fluctuations in particle trajectories as well as the aforementioned variations in individual snail behaviours. Nonetheless, our measurements are the first quantification of the flow field of the inhalant current, and they demonstrate that the snail is capable of producing a water current much larger in scale than its own body length.

To explore the flow field on the snail, we tracked food particles travelling on and into the funnel-shaped foot. Given the variability in the size and strength of different snails, we focused on the near-field flow data pertaining to one snail only. The particles on the foot slow down as they move over the horizontal part of the funnel prior to descending into its centre (figure 5a, b), contrary to the distant particles, which speed up as they approach the snail (figure 4a). This transition in flow behaviours is clearly shown in figure 4b. Figure 5c shows the time-elapsed trajectories of individual particles on the funnel; the trajectories correspond to a radially inward flow towards the centre of the funnel. Particles with similar radial coordinates on the foot showed no noticeable changes in speed with time, indicating that the fluid on the foot remained steady and thin.

We observed no noticeable change in the fluid level within the funnel over the duration of the feeding, suggesting that the mass of fluid is conserved. The region within the funnel does not fill up with water over time, implying that any water flowing into the centre of the foot must flow out from the funnel. To gain insight into this, we injected several drops of coloured dye until they filled the funnel to the top. The snail quickly responded by depleting the funnel and reestablishing the level of liquid to what it was before the dye injection. The coloured dye appeared to leak out on both sides of the snail along the adhering glass wall of the tank, as seen from above and from the side (see electronic supplementary material, videos S3 and S4, respectively). This suggests that any water flowing into the funnel recirculates back into the surrounding water and consequently maintains steady state.

3.2. Theory

The far-field flow needed to collect particles from a distance requires significant mechanical stresses to drive the flow around the snail. In order to sustain strong inward flow on the foot, the snail would have to maintain a fluid layer that remains sufficiently thin, particularly towards the edge as opposed to the centre of the foot. Otherwise, we would expect floating particles to be drawn in at slower speed as the fluid layer thickens over time, resulting in a decline in feeding performance. As we analyse theoretically below, it is non-trivial to maintain a thin fluid layer on the edge of the snail's foot. What plausible mechanisms could allow particles to continue flowing on the snail's foot, with the speed peaking at the edge of the foot as observed in the experiments?

We attempt to explore this problem with a simplified mathematical model that incorporates the basic physics of the system. The model is designed to predict the fluid thickness and surface velocity on the snail's foot, assuming the fluid arrives at the edge of the foot and leaves down the centre of the foot at some constant rate. Hence, it is reasonable to consider the centre of the foot as a point sink. The main purpose of the model is to identify plausible mechanisms that may account for the key experimental findings, focusing in particular on the trend that particles floating around the snail speed up as they approach the snail's foot and then slow down again on

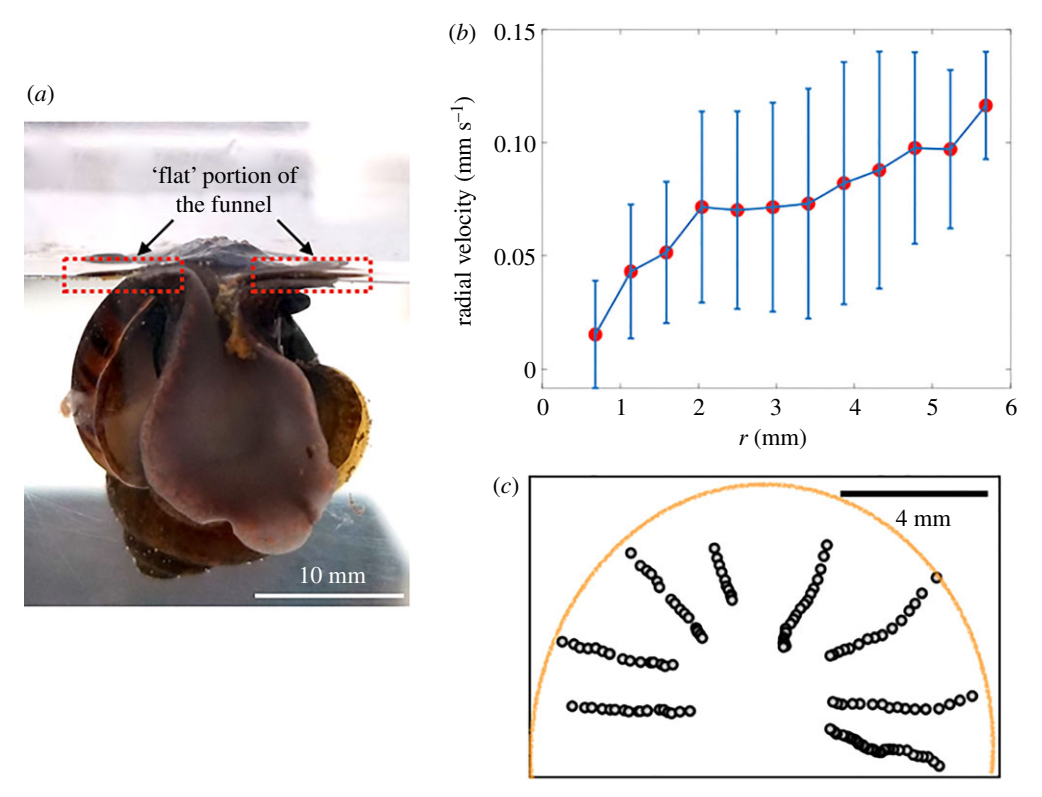


Figure 5. (a) The velocity data were taken from the flat horizontal portion of the funnel, and not from the food-storing centre. (b) Inward speed towards the funnel centre of particles on the snail's foot increases with their radial distance from the centre. Red symbols and error bars show the mean and standard deviation of velocities from 8 particle trajectories. (c) Particle trajectories on the flat part of the foot; time interval between two neighbouring circles is 1/29 s.

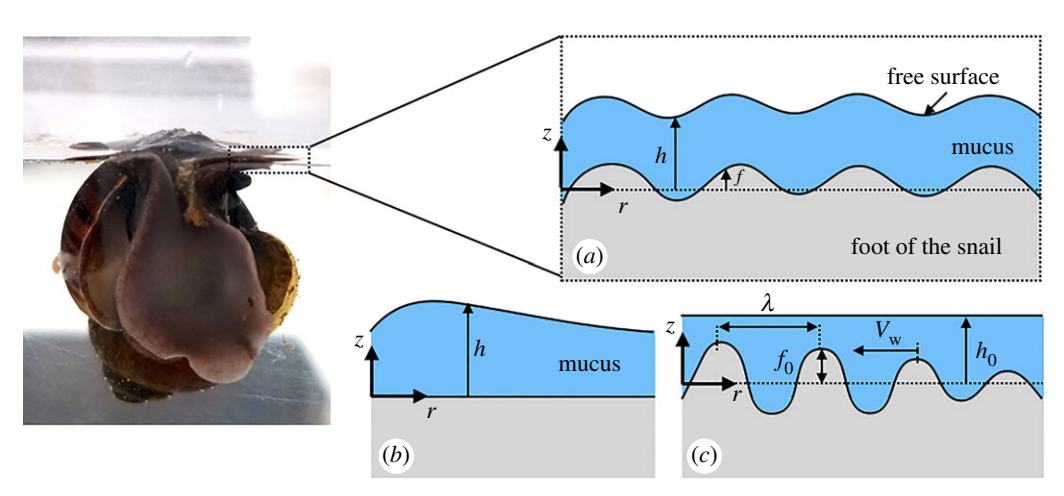


Figure 6. (a) Schematic of the mucous flow on the undulating foot of the snail. The shape of the foot is given by f, and the position of the free surface is denoted as h. The two simplified versions include (b) the flat surface of the snail foot, and (c) the periodic deformation of the snail foot while the interface of the mucous film remains flat.

the horizontal surface of the foot as they approach its centre. As demonstrated below, this will help in distinguishing whether the particles are sucked into the funnel or pumped along the undulating foot. We briefly discuss quantitative scalings of the speed with distance from the snail, though we are currently unable to validate any prediction against experimental data.

To explore plausible mechanisms of transporting food particles on the snail's foot, we developed a simplified model of the mucus flowing on the undulating foot. The model is based on the lubrication approximation, which is valid for a sufficiently thin mucous layer that is far thinner than the width of the foot. The model is similar in spirit to past models of mucus flowing adjacent to a crawling snail in a two-dimensional geometry [15], except that here we consider

an axisymmetric flow in the radially inward direction. There are several possible regimes that can arise depending on the relative importance of hydrostatic pressure, surface tension and active surface undulations. We consider each regime in turn below and suggest that undulation waves are most likely to be dominant in our experimental system, based on the observation that the food particles slow down as they move across the flat horizontal surface of the foot (figure 5) prior to descending down the funnel-shaped part of the foot.

As shown in figure 6a, f denotes the shape of the flat horizontal part of the snail foot, while h is the location of the free surface. Hence, h-f corresponds to the mucus thickness. We presently consider the viscous flow of the thin mucous film in the radially inward direction. Applying the lubrication

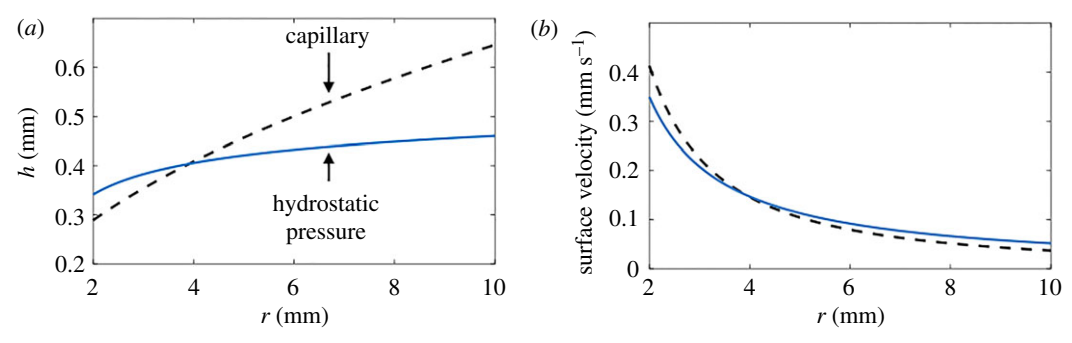


Figure 7. (a) The plot of the position of the free surface h as a function of r for the hydrostatic pressure-driven (solid blue) and capillary (dashed) flows. (b) The corresponding plot of surface velocity shows a decrease with r for both flow types.

approximation to the governing Navier–Stokes equations yields the following momentum equations in the *r*- and *z*-directions, respectively:

$$\frac{\partial p}{\partial r} = \mu \frac{\partial^2 u_r}{\partial z^2}, \quad \frac{\partial p}{\partial z} = -\rho g, \tag{3.1}$$

where u is the velocity component in the r-direction and p is the pressure. Here, ρ and μ correspond to the density and viscosity of the snail mucus, respectively, while g is the gravitational acceleration. Notably, at the free surface, z=h, we set $p=-\sigma(r^{-1}\partial h/\partial r+\partial^2 h/\partial r^2)$ to account for the pressure jump due to surface tension σ on the free surface. Combining equation (3.1) with the depth-averaged mass conservation leads to the following evolution equation for h:

$$\frac{\partial h}{\partial t} - \frac{1}{r} \frac{\partial}{\partial r} \left[r \frac{(h - f)^3}{3\mu} \left(\rho g \frac{\partial h}{\partial r} - \sigma \frac{\partial}{\partial r} \left(\frac{1}{r} \frac{\partial}{\partial r} \left(r \frac{\partial h}{\partial r} \right) \right) \right) \right] = 0.$$
(3.2)

Once h is found, it is straightforward to compute the free surface velocity as

$$u_r(z=h) = -\frac{(h-f)^2}{2\mu} \left[\rho g \frac{\partial h}{\partial r} - \sigma \frac{\partial}{\partial r} \left(\frac{1}{r} \frac{\partial}{\partial r} \left(r \frac{\partial h}{\partial r} \right) \right) \right]. \quad (3.3)$$

Instead of numerically solving equation (3.2) for h, we implement simplifying assumptions to test the importance of key physical effects that are present in the system. In particular, our focus is on deducing which physical mechanism may yield a free surface velocity that increases with r.

We compare the two terms that drive the flux inside the mucus film in equation (3.2)—the hydrostatic pressure gradient and surface tension—and consider the two contrasting limits. Based on equation (3.2), the hydrostatic term scales as $\rho gH/l$, and the capillary term is given by $\sigma H/l^3$, where H and l correspond to the characteristic mucus thickness and the typical wavelength of mucus deformations, respectively. Hence, the ratio between the two terms yields the Bond number $Bo = \rho g l^2/\sigma$. Based on the typical properties of mucus for which the ρ and σ values match those of water, Bo is varied from O(0.1) to O(10), when l is assumed to be 1 or 10 mm.

In the limit of $Bo \gg 1$, we first consider the flow inside the mucus that is driven by the hydrostatic pressure gradient, while neglecting the effects of surface tension. We also assume that any undulations of the snail foot are negligible compared to variations in the mucus thickness, such that f = 0, as illustrated in figure 6b; we consider the role of surface undulations later in the paper. This allows us to consider the

steady state, or $\partial h/\partial t = 0$, so that equation (3.2) becomes the following separable ordinary differential equation:

$$h^3 \frac{\mathrm{d}h}{\mathrm{d}r} = Q \frac{3\mu}{\rho g} \frac{1}{2\pi r},\tag{3.4}$$

where Q is the constant volume flow rate of the mucus, which is assumed to be positive for an inward flow. The resultant h profile is given by

$$h(r) = \left[h_0^4 + Q \frac{6\mu}{\pi \rho g} \ln \frac{r}{r_0} \right]^{1/4}, \tag{3.5}$$

where $h(r = r_0) = h_0$. Then, the corresponding free surface velocity is given by

$$u_r(z=h) = -\frac{3Q}{4\pi} \frac{1}{rh'},$$
 (3.6)

which must decrease with r. This result indicates importantly that, while hydrostatic pressure gradients alone may help drive the fluid layer on the snail's foot, the flow velocity would decay closer to the edge and induce minimal disturbance in the far field. This would not offer a viable strategy for collecting particles far away from the snail.

Another limit of interest is to focus on the effects of surface tension, while neglecting the hydrostatic pressure (i.e. $Bo \ll 1$). Then, in the steady-state limit, equation (3.2) reduces to

$$h^{3} \frac{\mathrm{d}}{\mathrm{d}r} \left(\frac{1}{r} \frac{\mathrm{d}}{\mathrm{d}r} \left(r \frac{\mathrm{d}h}{\mathrm{d}r} \right) \right) = -Q \frac{3\mu}{\sigma} \frac{1}{2\pi r},\tag{3.7}$$

which yields $h(r) = (4\mu Q/(\pi\sigma))^{1/4} r^{1/2}$ [17]. Then it follows that

$$u_r(z=h) = -\frac{3}{4\sqrt{2}} \left(\frac{\sigma}{\mu}\right)^{1/4} \left(\frac{Q}{\pi}\right)^{3/4} \frac{1}{r^{3/2}},$$
 (3.8)

so that the free surface velocity again decreases with r in contrast to the experimental observations.

For both hydrostatic pressure- and capillary-driven flows, values of h and $|u_r(z=h)|$ are plotted as a function of r in figure 7, based on the constant volumetric flow rate of $Q=1 \text{ mm}^3 \text{ s}^{-1}$. In addition, mucus is assumed to have the same density and surface tension as water, while being 100 times more viscous. Under those particular parameter values, the model results demonstrate that the mucus film thickens as a function of the distance from the centre of the funnel and is submillimetric in magnitude. The film thickness in the capillary-dominated flow grows faster than that in the hydrostatic pressure-dominated flow. Despite apparent differences in h, the corresponding surface velocities closely match between the two models, and the magnitude of the surface

royalsocietypublishing.org/journal/rsif *J. R. Soc. Interface* **17**: 20200139

velocity (i.e. $O(\text{mm s}^{-1})$) is consistent with the experimental values

However, contrary to the experimental observations, $|u_r(z=h)|$ decreases with the radial position r for both hydrostatic pressure- and capillary-driven flows. This discrepancy provides an important physical insight about the radially inward lubrication flows over a flat surface. Specifically, when a constant flow source is assumed either at the origin or the outer edge, the thickness of the film increases with r in the steady state, under the effects of hydrostatic pressure and surface tension. Hence, by mass conservation, the average velocity inside the fluid film must decrease with r, corresponding to a decrease in $|u_r(z=h)|$. This demonstrates that typical physical effects that govern the lubrication flow are insufficient to drive the radially inward flow that *increases* with r. In order to correctly capture the flow pattern created by a feeding snail, we must instead consider an alternative physical mechanism that drives the fluid flows across the funnel surface.

Next, therefore, we consider another plausible physical regime in which the mucus is driven by the active surface wave on the foot. Instead of sucking the mucus into the foot as considered above, the snail is now considered to pump the mucus along the foot surface. For simplicity, we assume that the surface wave has amplitude f_0 much smaller than its wavelength λ , which in turn is assumed to be much smaller than the characteristic radius of the funnel-shaped foot. At any instant the foot features multiple waves, with each wave assumed to travel radially inwards at speed V_w (figure 6c). For any pair of adjacent waves not too close to the centre of the foot, their crests occur at similar radial distances. This means that, if we move into the reference of the travelling wave, the axisymmetric geometry of the mucus flow can be approximated by a two-dimensional geometry, which greatly simplifies the analysis as presented below.

We expect the mucus to be driven primarily by surface waves and not so much by the effects of hydrostatic pressure and surface tension when the free surface remains approximately flat and undisturbed, that is, the location of the free surface h is approximately some constant h_0 . The free surface cannot be exactly equal to h_0 , otherwise the pressure would be uniform and there would be no flow on a no-slip surface. Of interest is the regime in which the free surface deflections are negligible compared to the amplitude of the foot undulation f_0 , assuming $f_0 < h_0$. This physical regime of an approximately flat free surface can be identified using scaling arguments. In the first governing equation of equation (3.1), viscous stresses $\mu \partial^2 u_r / \partial z^2$ arising from foot undulations can be at most of the order of $\mu V_w/(h_0-f_0)^2$, where V_w is the only radial velocity scale of the problem and $|h_0 - f_0|$ is the approximate thickness of the thinnest part of the mucus. This must be balanced by the pressure gradient $\partial p/\partial r$, which scales like either $\rho g \mid h - h_0 \mid /\lambda$ or $\sigma |h-h_0|/\lambda^3$, depending on whether hydrostatic pressure or surface tension is more important, respectively. This is because λ is the only length scale in the radial direction. By balancing the terms and rearranging, we find that the condition $|h - h_0| \ll f_0$ for an approximately flat free surface can be represented by

$$\frac{\rho g(h_0 - f_0)^2}{\sigma} \gg \frac{\lambda}{f_0} Ca, \quad Ca = \frac{\mu V_w}{\sigma} \ll \frac{(h_0 - f_0)^2 f_0}{\lambda^3}. \quad (3.9)$$

The free surface remains approximately flat provided that the capillary number Ca is sufficiently small. In this limiting regime, the open flow between the approximately flat free

surface and the undulating foot is equivalent to one half of the enclosed two-dimensional flow between two surfaces undulating with reflective symmetry, as considered in a model of peristalsis [18]. By symmetry, there is no tangential stress on the plane of symmetry, just as required on the approximately flat free surface of the original problem. More recent models of peristaltic pumping have considered the effect of introducing a particle in the fluid [19–22], but here we treat the small particles on the interface as tracers that do not modify the fluid flow.

We exploit the equivalence described above and make use of the main results from the earlier model of peristalsis [18]. For a fluid with no pressure variation at every periodic length $2\pi\lambda$, the time-averaged flux per unit width q is given by eqn (15) of [18]:

$$\theta = \frac{q}{V_w H_0} = \frac{3\phi}{2 + \phi^2},\tag{3.10}$$

which depends on the rescaled amplitude of the foot undulation $\phi = f_0/h_0$. The time-averaged velocity of a tracer particle on the free surface is given by

$$\frac{\Delta \xi}{1 + \Delta \xi} \tag{3.11}$$

according to eqn (40), where $\Delta \xi$ is the displacement of the particle every periodic cycle given by eqn (38) of [18]:

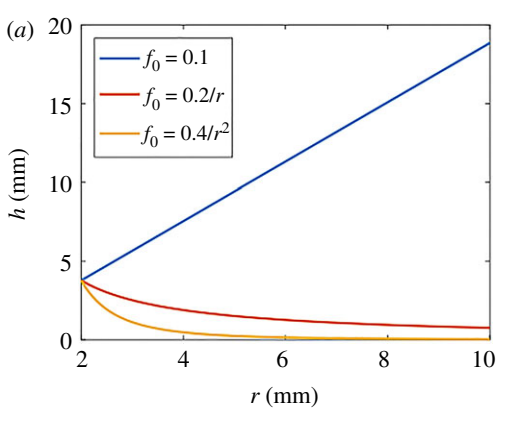
$$\Delta \xi = 3 \left(\frac{1 - \phi \theta}{\sqrt{\left(1 - \frac{3}{2}\phi \theta\right)^2 - \left(\frac{\phi}{2}\right)^2}} - 1 \right). \tag{3.12}$$

Given the mucus thickness h_0 , surface wave speed V_w and amplitude f_0 , we can use equation (3.10) to predict the rescaled flux θ and then equation (3.12) to predict the rescaled and time-averaged velocity of tracer particles on the mucus surface.

We apply the results above to the axisymmetric configuration of the feeding snail. Suppose the width-integrated flux $Q=2\pi rq$ remains steady at $1~{\rm mm}^3~{\rm s}^{-1}$ as assumed before. Equation (3.10) can be rearranged to obtain a quadratic equation for ϕ , which has two branches. For meaningful solutions with $\phi<1$, we must select the branch $\phi=k-\sqrt{k^2-2}$, where the dimensionless parameter $k=3\pi r~V_w~f_0/Q$ must be sufficiently large for $\phi<1$. To predict how the mucus thickness h_0 and surface velocity change with radial distance r, we prescribe the surface wave speed V_w and amplitude H_0 , which must be under the control of the snail.

Here, we consider three different ways of varying the surface wave amplitude, assuming the wave speed remains steady at $V_w = 20 \text{ mm s}^{-1}$. If the amplitude is constant, e.g. $f_0 = 0.1 \text{ mm}$, the mucus is thicker at larger distance r and the tracer particle moves more slowly there as plotted in figure 8a,b). But if the amplitude decays sufficiently quickly with r, e.g. r^{-2} , the mucus gets thinner and the tracer particles move more quickly at larger r as observed experimentally. This demonstrates a plausible mechanism consistent with experiments. The advantage of this mechanism is that a strong flow speed arises near the edge of the foot, which is suitable for inducing a strong far-field flow needed to collect distant particles floating around the snail.

We briefly discuss some possible effects of the near-field mucus flow on the bulk water flow in the far field. First, the thin fluid flow on the snail may undulate the air-water



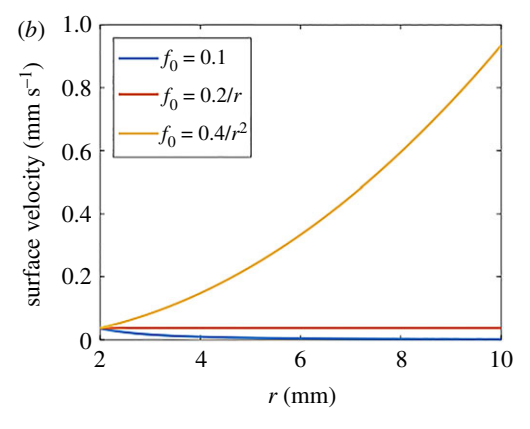


Figure 8. Steady film thickness (a) and surface velocity (b) profiles on an undulating foot, assuming the undulation amplitude f_0 is uniform or decays linearly or quadratically with distance r.

interface and consequently transport floating particles, e.g. due to Stokes drift in the direction of the travelling disturbance [23]. However, any disturbance from the snail is expected to radiate outwards and drive particles in the opposite direction to the observed inward flow. Distortions of the air—water interface are unlikely to be playing any major role, given that the shape of the interface appeared to be flat and horizontal in the region away from the snail. Second, Marangoni stresses on the interface may drive a directional flow [24] or a radially outward flow [25], with the flow carrying significant momentum in a thin boundary layer along the interface. However, the snail generates a relatively weak and radially inward flow, which would drive the flow not only near the interface but also in the bulk fluid.

To illustrate the types of bulk flows that may arise in the far field, we consider two extreme cases in the absence of either viscosity or inertia, corresponding to the limits of high or low Reynolds number, respectively. In either case, we assume the air-water interface remains approximately horizontal and consider axisymmetric flow along the interface. This arises provided that the effects of any confining boundaries are neglected for simplicity, and that the far-field flow is driven primarily by mechanical stresses at the edge of the snail's foot. In the inviscid limit, the effect of the snail's foot on the far-field flow could be represented by a source quadrupole in potential theory, equivalent to having point sinks distributed along the perimeter of a circular foot in the horizontal plane, with a point source centred inside the circle to conserve mass. In the viscous limit, the snail's inhalant current may be represented by a stresslet or force dipole. The far-field flow is expected to decay with distance r like r^{-4} in the inviscid limit or r^{-2} in the viscous limit. Either way, the key ingredient for driving a strong far-field flow is to generate strong flow or mechanical stress at the edge of the snail's foot, with the induced flow expected to decay more slowly in the viscous limit.

4. Conclusion

Downloaded from https://royalsocietypublishing.org/ on 09 July 2021

In this study, we investigated the pedal surface collecting mode of feeding by apple snails, by combining biological experiments and mathematical modelling. Our experiments consisted of isolating one apple snail inside a water-filled tank and creating a conducive environment for the snail to search for food on the water surface. After varied periods of time, the snail attached itself on a tank wall with the posterior part of its foot, while its anterior part formed a funnel. The funnel was shaped in such a way that its largest opening sat near the air-water interface. Then, the snail generated a surface current that pulled the food particles into the funnel. In addition to the qualitative observations of the snail's feeding behaviour, we experimentally measured the inhalant flow field, by tracking the motion of individual food particles. Because of the low Stokes number, the particle velocities represent the fluid velocities at the air-water interface. Our measurements revealed two striking features. First, the velocity on the water surface decays very slowly as a function of the radial distance r from the funnel centre in the far field. This slow decay outside the funnel cannot be explained by the inviscid or viscous flow theory. Second, over the funnel surface, the surface velocity increased with r, reaching the maximum value at the outer edge of the funnel. This transition in surface velocity inside and outside the funnel points to the existence of distinct physical mechanisms and boundary conditions that must govern the near- and far-field flows.

To help rationalize the near-field flow, we developed a mathematical model of the flow over the funnel surface. Based on the observations of [15], we assume that there is a thin film of mucus on the upturned surface of the snail's foot and employ lubrication approximations to describe the thin film flow. In the first two limiting cases, we assume that the funnel surface remains flat, while the flow is driven by the hydrostatic pressure gradient or surface tension. The simple assumptions allow us to derive analytical solutions for the coupled mucus thickness and surface velocity. However, the results demonstrate that the surface velocity decreases with r, which does not match the velocity measurements. This discrepancy suggests that an idealized lubrication flow over a flat surface that is driven radially inward by a source is incompatible with the flow generated by a feeding snail. Finally, we hypothesize that the mucus flow may be driven by surface undulations and derive scaling relationships in the limit where the fluid-fluid interface remains approximately flat. This model allows for the surface velocity to increase with r under certain parameter regimes, pointing to the potential mechanism that enables the observed food collection on the fluid-fluid interface. We also examined that the farfield flow driven by stresses at the edge of the funnel would drive a radially inward flow that decays with r, whether it is in the inviscid or viscous flow limits.

The present study is only the first step towards gaining a full understanding of this mode of apple snail feeding.

royalsocietypublishing.org/journal/rsif *J. R. Soc. Interface* **17**: 20200139

While the current experimental data show clear trends in flow fields, they exhibit a considerable scatter inherent in experiments with biological organisms. Furthermore, the current experiments do not provide information about the detailed motion of the funnel or the thickness of the mucous film. Hence, additional experiments on the flow field, free surface shapes, and the mucous film would be required to understand the fluid mechanics underlying apple snail feeding on the free surface. A possible method for measuring the mucous deformation would be to project a laser sheet at an angle and then measure the reflected image [26]. In addition to more measurements, a more detailed lubrication model is needed to fully couple the muscular undulations or ciliary motion with the free surface shape. Our preliminary model suggests that inward mucus pumping may be maximized when the free surface shape remains approximately flat. Finally, a mathematical model for the far-field flow is needed to explain the fluid mechanics underlying the current experimental observations.

Ethics. Institutional guidelines for research on invertebrates were followed

Data accessibility. Experimental data are available as electronic supplementary material.

Authors' contributions. So.J., Su.J., S.L., R.C. and D.T. conceived of and designed the study. So.J. generated the experimental data. Su.J, S.L. and D.T. analysed the data and developed the mathematical model. So.J., Su.J., S.L., R.C. and D.T. drafted the manuscript and gave final approval for publication.

Competing interests. The authors declare no competing interests.

Funding. This work was partly supported by the National Science Foundation (CBET-1919753 to Su.J., CBET-1605947 to S.L., and CBET-1603929 to D.T.) and the US Army Research Office (W911NF-17-1-0442 to D.T.).

Acknowledgements. Contribution number 10933 of the University of Hawaii School of Ocean and Earth Science and Technology.

References

- Speiser B. 2001 Food and feeding behaviour. In *The biology of terrestrial molluscs* (ed. GM Barker), pp. 259–288. Wallingford, UK: CABI Publishing.
- Keller HW, Snell KL. 2002 Feeding activities of slugs on Myxomycetes and macrofungi. *Mycologia* 94, 757–760. (doi:10.1080/15572536.2003.11833169)
- Mason CF. 1970 Snail populations, beech litter production, and the role of snails in litter decomposition. *Oecologia* 5, 215–239. (doi:10.1007/ BF00344885)
- Lombardo P, Cooke GD. 2002 Consumption and preference of selected food types by two freshwater gastropod species. *Archiv für Hydrobiologie* 155, 667–685. (doi:10.1127/archiv-hydrobiol/155/2002/667)
- Hayes KA et al. 2015 Insights from an integrated view of the biology of apple snails (Caenogastropoda: Ampullariidae). Malacologia 58, 245–303. (doi:10.4002/040.058.0209)
- Cowie RH. 2001 Can snails ever be effective and safe biocontrol agents? *Int. J. Pest Manage.* 47, 23–40. (doi:10.1080/09670870150215577)
- Meyer WM III, Hayes KA, Meyer AL. 2008 Giant African snail, Achatina fulica, as a snail predator. Am. Malacological Bull. 24, 117–120. (doi:10.4003/ 0740-2783-24.1.117)
- Mackenstedt U, Märkel K. 2001 Radular structure and function. In *The biology of terrestrial molluscs* (ed. GM Barker), pp. 213–236. Wallingford, UK: CABI Publishing.

- Cazzaniga N, Estebenet A. 1984 Revisión y notas sobre los hábitos alimentarios de los Ampullariidae (Gastropoda). Historia Natural 4, 213–224.
- Saveanu L, Martín PR. 2013 Pedal surface collecting as an alternative feeding mechanism of the invasive apple snail *Pomacea canaliculata* (Caenogastropoda: Ampullariidae). *J. Molluscan Stud.* 79, 11–18. (doi:10.1093/mollus/eys030)
- 11. Johnson B. 1952 Ciliary feeding in *Pomacea paludosa*. *Nautilus* **66**, 1–5.
- Cheesman D. 1956 The snail's foot as a Langmuir trough. Nature 178, 987–988. (doi:10.1038/178987b0)
- Saveanu L, Martín PR. 2015 Neuston: a relevant trophic resource for apple snails? *Limnologica* 52, 75–82. (doi:10.1016/j.limno.2015.03.005)
- 14. Declerck CH. 1995 The evolution of suspension feeding in gastropods. *Biol. Rev.* **70**, 549–569. (doi:10.1111/j.1469-185X.1995.tb01651.x)
- Lee S, Bush JW, Hosoi A, Lauga E. 2008 Crawling beneath the free surface: water snail locomotion. Phys. Fluids 20, 082106. (doi:10.1063/1.2960720)
- 16. Brown D. 2017 Tracker, video analysis and modeling tool (computer software).
- Zheng Z, Fontelos MA, Shin S, Dallaston MC, Tseluiko D, Kalliadasis S, Stone HA. 2018 Healing capillary films. J. Fluid Mech. 838, 404–434. (doi:10.1017/jfm.2017.777)
- Shapiro AH, Jaffrin MY, Weinberg SL. 1969
 Peristaltic pumping with long wavelengths at low

- Reynolds number. *J. Fluid Mech.* **37**, 799–825. (doi:10.1017/S0022112069000899)
- Hung T-K, Brown TD. 1976 Solid-particle motion in two-dimensional peristaltic flows. *J. Fluid Mech.* 73, 77–96. (doi:10.1017/S0022112076001262)
- Fauci LJ. 1992 Peristaltic pumping of solid particles. *Comput. Fluids* 21, 583–598. (doi:10.1016/0045-7930(92)90008-J)
- 21. Takagi D, Balmforth N. 2011 Peristaltic pumping of rigid objects in an elastic tube. *J. Fluid Mech.* **672**, 219–244. (doi:10.1017/S0022112010005926)
- 22. Blanchette F. 2014 The influence of suspended drops on peristaltic pumping. *Phys. Fluids* **26**, 061902. (doi:10.1063/1.4882263)
- Punzmann H, Francois N, Xia H, Falkovich G, Shats M. 2014 Generation and reversal of surface flows by propagating waves. *Nat. Phys.* 10, 658–663. (doi:10.1038/nphys3041)
- Bandi M, Akella V, Singh D, Singh R, Mandre S. 2017 Hydrodynamic signatures of stationary Marangonidriven surfactant transport. *Phys. Rev. Lett.* 119, 264501. (doi:10.1103/PhysRevLett.119.264501)
- Mandre S. 2017 Axisymmetric spreading of surfactant from a point source. J. Fluid Mech. 832, 777–792. (doi:10.1017/jfm.2017.708)
- Vella D, Bico J, Boudaoud A, Roman B, Reis PM. 2009
 The macroscopic delamination of thin films from elastic substrates. *Proc. Natl Acad. Sci. USA* 106, 10 901–10 906. (doi:10.1073/pnas.0902160106)